Plume Statistics in Thermal Turbulence: Mixing of an Active Scalar

Sheng-Qi Zhou and Ke-Qing Xia*

Department of Physics, The Chinese University of Hong Kong, Shatin, Hong Kong, China

(Received 15 July 2002; published 15 October 2002)

Statistical properties of the temperature field in turbulent convection are studied experimentally. We show that the skewness of the plus and minus temperature increments can be used to quantitatively characterize the mixing zone in the convective flow and the result reveals how the mixing zone evolves with the Rayleigh number. We also present evidence for the saturation of the temperature structure function exponent and that the saturation is related to thermal plumes. A more direct study of the thermal plumes suggests that their sizes have a distribution that is approximately log-normal.

DOI: 10.1103/PhysRevLett.89.184502 PACS numbers: 47.27.Qb, 44.25.+f

In the problem of turbulent convection the temperature field is in general an active scalar, but it shows certain features similar to those of a passive one. This is because both obey similar diffusion-advection equations and the difference is that in the active case the advecting velocity field is influenced by the advected scalar. Thus applying some of the analysis methods developed for passive scalars [1,2] to the temperature field in thermal convection may help us gain insight into the convection problem and may also provide the passive scalar problem itself a different perspective. A sealant feature of passive scalar mixing is the persistence of nonzero skewness of the scalar derivatives, which invalidates the local isotropy assumption of the classical Kolmogorov-Obukhov-Corrsin theory of passive scalars [3]. The nonzero skewness is believed to be due to sharp fronts or gradients of the scalar, which manifest as cliffs and ramps in its time series. In turbulent convection, thermal plumes are the predominant coherent structures that transport heat and drive the flow. These mushroomlike objects consist of a cap with sharp temperature gradient and a stem that is relatively diffusive, so one would imagine that plumes would generate cliff-ramp-like structures when passing a thermal detector, analogous to the behavior of sharp fronts in passive scalars.

This Letter reports an experimental investigation of the small-scale statistical properties of an active scalar—the temperature field in thermal convection and how this quantity is different from or similar to generic passive scalars. The experiment is conducted in a Rayleigh-Bénard convection cell filled with water. Details of the cell are described in Ref. [4], briefly it is a vertical cylinder of height $L = 19.6$ cm and diameter 19 cm, with upper and lower copper plates and Plexiglas sidewall. The temperature measurement has been described before [5]; in the current paper new measurements have been made to acquire temperature records systematically as functions of the Rayleigh number Ra and of the position z from cell bottom (at Prandtl number Pr$\simeq$ 4). Typical time series consists of (1–4) $\times 10^6$ data points with sampling rate ranging from 16 to 128 Hz.

We first examine the statistical properties of the plus and minus temperature increments [6], which are defined as $\delta_\tau T^\pm = (|\delta_\tau T| \pm \delta_\tau T)/2$, where $\delta_\tau T = T(t+\tau) - T(t)$ is the temperature increment over a time τ. Figure 1 shows the skewness $S(\delta_\tau T^\pm) = \langle(\delta_\tau T^\pm)^3\rangle/\langle(\delta_\tau T^\pm)^2\rangle^{3/2}$ as a function of the scale τ and in three regions of the convection cell. In the figure, τ is normalized by the Bolgiano time τ_B(corresponding to the Bolgiano length l_B), which is determined experimentally from the normalized second order structure function (from which we also obtain the dissipation time τ_d corresponding to the Kolmogorov scale η) [5]. Figure 1 shows that $S(\delta_\tau T^+)$ and $S(\delta_\tau T^-)$ are essentially the same at positions near the thermal boundary layer ($z = 1.6$) and in the central

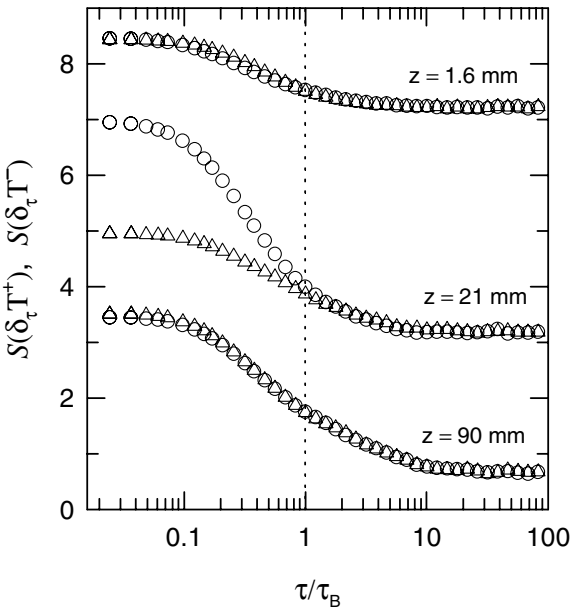

FIG. 1. A semilog plot of the skewness of the plus (circles) and minus (triangles) temperature increments as functions of the scale τ measured at Ra $= 1.8 \times 10^{10}$ and for three values of z. For clarity, the $z = 90$ data are shifted down by 2 and $z = 1.6$ data shifted up by 4.

region ($z = 90$), whereas in the intermediate region $S(\delta_\tau T^+)$ is larger than $S(\delta_\tau T^-)$ for $\tau < \tau_B$ and the difference increases with decreasing scale. This may be understood from the properties of thermal plumes. When a (hot) plume passes through a thermal detector, it would produce a spike with a steep rising edge (due to its cap) and a relatively gentle falling edge (due to its tail) in the temperature time series. The plus and minus temperature increments capture, respectively, the slope of the rising and falling edges for τ smaller than the size of a plume (in the time domain). Figure 1 indicates that $S(\delta_\tau T^+)$ and $S(\delta_\tau T^-)$ start to separate from τ_B and the difference reaches maximum around τ_d ($= 0.05\tau_B$ in this case). This suggests that the cap thickness of a typical plume should be smaller than l_B but larger than η (more evidence is below). For $\tau > \tau_B$, features smaller than the corresponding scale are averaged out, resulting in the same values for the plus and minus skewness. Note that the data are measured in the lower half of the convection cell where hot plumes dominate and thus $S(\delta_\tau T^+)$ is greater than $S(\delta_\tau T^-)$ in this region. The results for $z =$ 1.6 and 90 may be understood by the fact that there are few plumes near the boundary layer and in the cell center.

For small-scale behavior we study the statistics of temperature time derivative $\partial T/\partial t$, which can be approximated by $\delta_\tau T$ for $\tau \leq \tau_d$ [2]. We denote $S^{\pm}_{\partial T} \equiv S(\partial T^{\pm}/\partial t)$ as the skewness for the "plus" and "minus" temperature derivatives, and we study how they change with position and evolve with Ra, as shown in Fig. 2. The figure reveals three distinct regions in the convection cell. First is the central core in which $S^+_{\partial T}$ and $S^-_{\partial T}$ are the same and change very little with position (for large Ra). We also find that the "total" skewness $S_{\partial T}$ of the temperature derivative in this region is nearly constant and close to zero. Thus temperature fluctuations in this region may be regarded as statistically homogeneous and locally isotropic. Second is the region inside the thermal boundary layer in which $S^+_{\partial T}$ and $S^-_{\partial T}$ are roughly the same but not a constant of the position. In the intermediate region $S^+_{\partial T}$ is larger than $S^-_{\partial T}$, signifying the presence of hot plumes. This is the region where plumes are stretched, mixed, and swept by the velocity field and corresponds to the so-called mixing zone first proposed to explain the hard convective turbulence [7]. Figure 2 thus reveals how the mixing zone evolves and the central core grows with Ra: for a value of Ra as high as 5×10^8, a central core as defined above hardly exists and the mixing zone occupies most of the cell, this is despite the fact that the fluid's motion is already one decade into the hard turbulence state; as Ra increases the mixing zone shrinks and the central core grows but not until Ra reaches very high values do we have a sizable homogeneous and isotropic central region, which takes up roughly 50% of the cell at $\mathrm{Ra} = 1 \times 10^{10}$ (from $z/L = 0.25$ to 0.75, assuming top-bottom symmetry). The skewness profiles in Fig. 2 also provide a quantitative way to characterize the mixing zone, it is the region where a gap exists between $S^+_{\partial T}$ and $S^-_{\partial T}$. The inset of Fig. 2(c) shows the scaling of the mixing zone's upper and lower edges with Ra. For comparison, the directly measured thermal boundary layer thickness and the theoretically predicted size of the mixing zone $l_m/L = 2\mathrm{Ra}^{-1/7}$ [8] are also plotted. The figure shows clearly that the lower edge of the mixing zone indeed corresponds to the thermal boundary layer. For the upper edge, the experimental result gives an exponent of $-(0.13 \pm 0.02)$ which is consistent with the theoretical value of $-1/7$. Since the theoretical prediction is based on scaling argument, it is perhaps not surprising that the magnitudes of the two are not the same. We point out that an earlier study also revealed that profiles of temperature derivative skewness reach maximum values outside the thermal boundary layer and the authors referred this region as the mixing zone, but it was not characterized quantitatively [9].

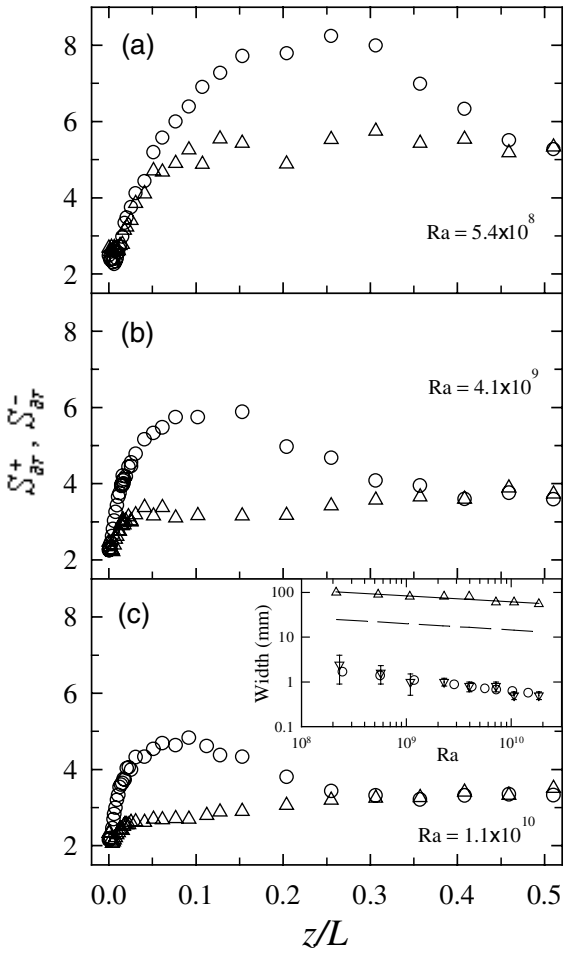

FIG. 2. Skewness of the plus (circles) and minus (triangles) temperature derivatives as functions of the scaled distance z/L and for three values of Ra. Inset: Ra dependence of the upper (triangles) and lower (inverted triangles) edges of the mixing zone, the thermal boundary layer (circles), and theoretical value (dashed line) for the mixing zone.

A prominent feature of passive scalars is the saturation of exponents of the high order structure functions (the exponent ζ_n for structure function of order n approaches a constant ζ_∞ for large enough n) [10,11], which is believed to be caused by the cliffs or fronts [10,12]. A recent numerical study of two-dimensional (2D) thermal convection also shown evidence for saturation of the temperature structure function exponents [13]. But there is so far no experimental verification of this. To test this experimentally, we acquired a few extra-long temperature records that contain 1.2×10^8 data points (at a sampling rate of 128 Hz). The measurements are made at Ra $= 1.8 \times 10^{10}$ and simultaneously at two positions in the cell, one at the center and the other 2 cm from the sidewall at midheight and is within the plane of the large scale circulation. Shadowgraphs show that the sidewall point is much more abundant in plumes than the center point, so results from the two points may give us a clue about the relationship between plumes and saturation. As pointed out by Celani *et al.* [10], saturation of the exponents is equivalent to the PDF of temperature increments in the inertial range having the form $P(\delta_\tau T) = \tau^{\zeta_\infty} Q(\delta_\tau T/T_{\rm rms})$ for $\delta_\tau T$ sufficiently larger than $T_{\rm rms} = \langle (T - \langle T \rangle)^2 \rangle^{1/2}$, where Q is a universal function. Because high order structure functions are very sensitive to the far tails of the PDF, collapsing of the scaled PDF $\tau^{-\zeta_\infty} P(\delta_\tau T)$ is a statistically more reliable test of the saturation [10,12]. Figure 3 shows the scaled PDF vs normalized temperature increments for several values of the separation scale τ within the inertial range (in this case the buoyancy subrange [5]): (a) cell center and (b) sidewall. It is clear that at the sidewall position there is a collapse of the PDFs for $\delta_\tau T \gtrsim 5T_{\rm rms}$ and there is no collapse for the center point, providing a strong indication that the saturation is caused by plumes. To rule out the possibility that the center position might have a different saturation exponent ζ_∞ than the sidewall point, we have tried various values other than 0.8 but still could not obtain satisfactory collapse of the PDFs. Note that the PDFs in Fig. 3 become noisy for $\delta_\tau T > 10T_{\rm rms}$, such values of $\delta_\tau T$ represent highly improbable and extremely large excursions of the temperature field and the current data clearly do not have sufficient statistics to verify the collapsing beyond $10T_{\rm rms}$.

A further test of the saturation phenomenon is to examine the cumulated probabilities $\int_{\delta_\tau T}^{\infty} P d(\delta_\tau T)$ as a function of τ for $\delta_\tau T$ exceeding certain threshold $\lambda T_{\rm rms}$ [10]. The results are shown in Fig. 4 for several values of λ, with the inset showing the compensated probabilities. The figure shows that the cumulated probabilities become parallel to each other in the buoyancy subrange ($\tau > \tau_B$) when $\delta_\tau T$ exceeds $5T_{\rm rms}$ and the compensated plots indicate that the saturation exponent for the active scalar in 3D is indeed $\zeta_\infty = 0.8$, consistent with 2D numerical result. It is interesting to note that in the passive scalar case ζ_∞ also has the same value (≈ 1.4) for both 3D experiment [11] and 2D simulations [10]. On the other hand, we note that in the 2D numerical studies of both passive [10] and active [13] scalars the collapsing of the PDFs occur when the temperature increment $\delta_\tau T \gtrsim (2\text{–}3)T_{\rm rms}$, in contrast to $\delta_\tau T \gtrsim 5T_{\rm rms}$ for our case. This implies that the temperature field in turbulent convection is more intermittent than a passive scalar.

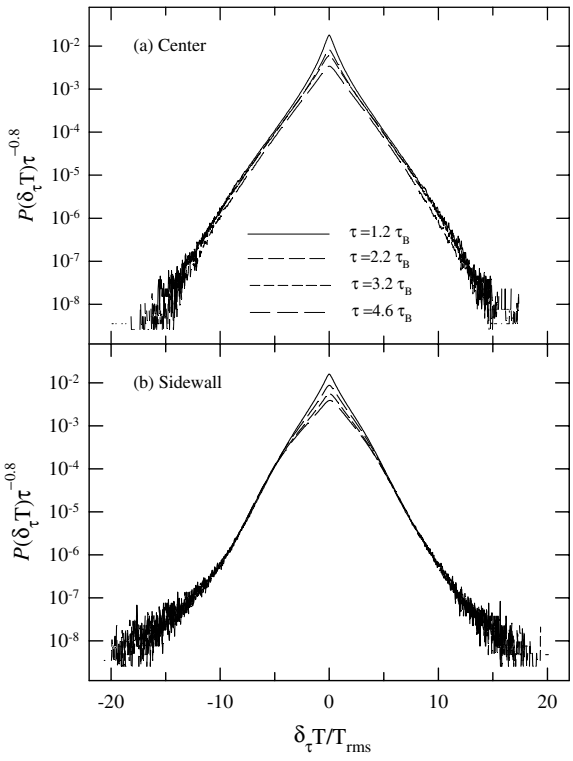

FIG. 3. Scaled PDF vs normalized temperature increments for several inertial range values of τ [same for (a) and (b).]

A more direct way to study the statistics of the thermal plumes is to think of them as cliff-ramp structures, as in passive scalars. Here we use a criterion to identify cliffs in

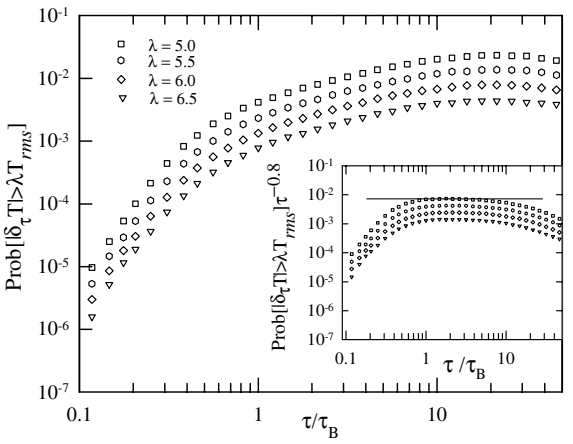

FIG. 4. Cumulated probabilities for $\delta_\tau T > \lambda T_{\rm rms}$ for several values of λ and for the sidewall data. The inset shows the compensated probabilities with the $\zeta_\infty = -0.8$.

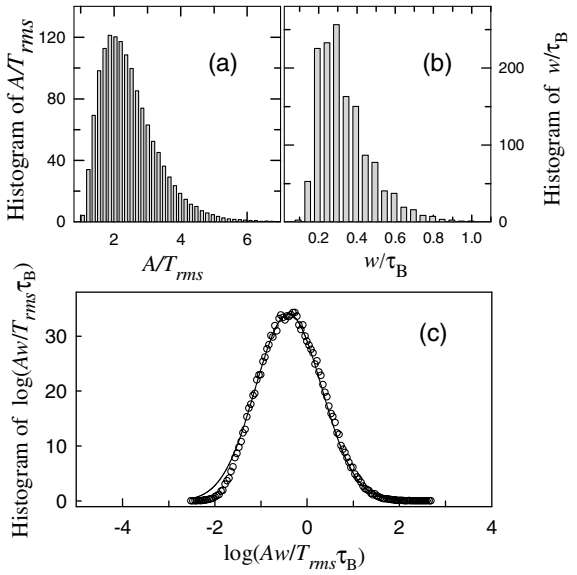

FIG. 5. Histograms of (a) cliff amplitude, (b) cliff width, and (c) the logarithm of normalized "plume" size, the solid line indicates a log-normal distribution. All vertical axes have been scaled by 100.

temperature time series that is similar to the one used for passive scalar [11]: a "cliff" is identified when $\delta_{\tau_d} T > T_{\rm rms}$, where $\delta_{\tau_d} T$ is the temperature increment over the dissipation scale τ_d. When such a cliff is found, its position t_0 is defined as the point where temperature change is most steep, its amplitude A as the difference between the two temperature extrema surrounding t_0, and its width w the separation in time between the two extrema. Applying this procedure to the extra-long sidewall temperature series, we identified 140 000 cliffs. Figure 5 shows the histograms of the normalized amplitude $A/T_{\rm rms}$ and width w/τ_B of the extracted cliffs, which indicate that A and w peak around $2T_{\rm rms}$ and $0.25\tau_B$, respectively [14]. If we associate the extracted cliff with the cap of a plume, then it means that the most probable temperature jump across the cap of a plume is about $2T_{\rm rms}$ and the most probable thickness of a cap is about $0.25 l_B$ ($\approx 5\eta$). We find that A, w, and their product all have approximate log-normal distributions. Figure 5(c) shows the histogram of the log of the normalized product $Aw/T_{\rm rms}\tau_B$, with the solid line showing a log-normal distribution. If we take Aw to be proportional to the "heat content" or "size" of a plume, then this suggests that plumes have approximate log-normal distribution. To verify that the extracted "plumes" are indeed responsible for the anomalous behavior of the skewness in the mixing zone, we applied the same procedure to temperature data in that region and remove the identified cliffs from the temperature time series and then recalculate $S^+_{\partial T}$ and $S^-_{\partial T}$. We find that in this case the gap between $S^+_{\partial T}$ and $S^-_{\partial T}$ shrinks considerably, suggesting that the mixing zone is indeed a region dominated by plumes.

To summarize, we have demonstrated that the skewness of the plus and minus temperature increments can be used to precisely characterize the mixing zone and to study the local anisotropy of the temperature field in turbulent convection. The evolution of the mixing zone with Rayleigh number shows how a homogeneous and isotropic region in the convection cell emerges as Ra increases; this region hardly exists at Ra $\approx 5 \times 10^8$ and takes up roughly half of the cell volume at Ra $\approx 1 \times 10^{10}$. If thermal plumes can be identified as cliffs in temperature time series, then our result suggests that the plumes have a distribution that is close to log-normal. We also find evidence for the saturation of the exponents of high order temperature structure functions, and that this saturation may be attributed to the presence of plumes. This suggests that exponent saturation is a generic feature not limited to passive scalars and exists whenever there are sharp fronts in the random field.

We thank E. Ching, K. Sreenivasan, and P. Tabeling for stimulating discussions and gratefully acknowledge support of this work by a grant from Hong Kong Research Grants Council (Project No. CUHK 4224/99P).

*Corresponding author.
Email address: kxia@phy.cuhk.edu.hk

[1] B. I. Shraiman and E. D. Siggia, Nature (London) **405**, 639 (2000).
[2] Z. Warhaft, Annu. Rev. Fluid Mech. **32**, 203 (2000).
[3] K. R. Sreenivasan, Proc. R. Soc. London A **434**, 165 (1991).
[4] S.-L. Lui and K.-Q. Xia, Phys. Rev. E **57**, 5494 (1998).
[5] S.-Q. Zhou and K.-Q. Xia, Phys. Rev. Lett. **87**, 64501 (2001).
[6] The plus and minus structure functions were first introduced to study ramp structures of the velocity field in Navier-Stokes turbulence by S. I. Vainshtein and K. R. Sreenivasan [Phys. Rev. Lett. **73**, 3085 (1994)].
[7] B. Castaing *et al.*, Fluid Mech. **204**, 1 (1989).
[8] I. Procaccia *et al.*, Phys. Rev. A **44**, 8091 (1991).
[9] A. Belmonte and A. Libchaber, Phys. Rev. E **53**, 4893 (1996).
[10] A. Celani, A. Lanotte, A. Mazzino, and M. Vergassola, Phys. Rev. Lett. **84**, 2385 (2000).
[11] F. Moisy, H. Willaime, J. S. Andersen, and P. Tabeling, Phys. Rev. Lett. **86**, 4827 (2001).
[12] A. Celani, A. Lanotte, A. Mazzino, and M. Vergassola, Phys. Fluids **13**, 1768 (2001).
[13] A. Celani, A. Mazzino, and M. Vergassola, Phys. Fluids **13**, 2133 (2001).
[14] We also used several other thresholds for the cliffs, i.e., $\delta_{\tau_d} T > 3T_{\rm rms}$ and $5T_{\rm rms}$, and find that the most probable cliff width is always around $0.25\tau_B$ but the most probable amplitude shifts to higher values when the threshold is increased since events of lower "intensity" are excluded. The shapes of the various histograms also remain invariant for different thresholds.